The impact of dehydration and extremely low HCl values in the Antarctic stratospheric vortex in mid-winter on ozone loss in spring

Yiran Zhang-Liu[1], Rolf Müller[1,5], Jens-Uwe Grooß[1,5], Sabine Robrecht[1,2], Bärbel Vogel[1,5], Abdul Mannan Zafar[1,3], and Ralph Lehmann[4]

[1]Institute of Energy and Climate Research (IEK-7), Forschungszentrum Jülich, Jülich, Germany
[2]Deutscher Wetterdienst, Offenbach, Germany
[3]Biotechnology Research Center, Technology Innovation Institute, Masdar City, Abu Dhabi, United Arab Emirates
[4]Alfred Wegener Institute, Helmholtz Centre for Polar and Marine Research, Potsdam, Germany
[5]Center for Advanced Simulation and Analytics (CASA), Forschungszentrum Jülich, Jüich, Germany

Correspondence: Rolf Müller (ro.mueller@fz-juelich.de) and Yiran Zhang-Liu (yiranz.luna@gmail.com)

Abstract. Simulations of Antarctic chlorine and ozone chemistry show that in the core of the Antarctic vortex (16–18 km, 85–55 hPa, 390–430 K) HCl null cycles (initiated by reactions $CH_4 + Cl$ and $CH_2O + Cl$) are effective. These HCl null cycles allow HCl mixing ratios to remain very low throughout Antarctic winter and ozone destroying chlorine (ClO_x) to remain enhanced, so that rapid ozone depletion proceeds. Sensitivity studies show that the reaction $CH_3O_2 + ClO$ is important for the efficacy of the HCl null cycle initiated by the reaction $CH_4 + Cl$ and that using the current kinetic recommendations instead of earlier ones has little impact on the simulations. Dehydration in Antarctica strongly reduces ice formation and the uptake of HNO_3 from the gas phase; however the efficacy of HCl null cycles is not affected. Further, the effect of the observed very low HCl mixing ratios in Antarctic winter are considered; HCl null cycles are efficient in maintaining low HCl (and high ClO_x) throughout Antarctic winter. All simulations presented here for the core of the Antarctic vortex show extremely low minimum ozone values (below 50 ppb) in late September/early October in agreement with observations.

1 Introduction

The Antarctic ozone hole is a phenomenon of substantially reduced polar ozone that has reoccurred every winter and spring over Antarctica since about four decades (Jones and Shanklin, 1995; Müller et al., 2008; Bodeker and Kremser, 2021; WMO, 2022; Klekociuk et al., 2022; Johnson et al., 2023). In many years, the Antarctic ozone hole shows a broad altitude region of very low ozone in the altitude region of 14-21 km (∼ 380-550 K) (Solomon et al., 2005; Jurkat et al., 2017; Johnson et al., 2023). In exceptional years, sudden stratospheric warmings occur in the Antarctic (2002 and 2019) causing unusually low ozone depletion (e.g. Müller et al., 2008; Grooß et al., 2005; Smale et al., 2021). Substantial polar ozone loss may also occur in the Arctic; albeit the ozone loss shows a much stronger year-to-year variability (e.g., Müller et al., 2008; Johansson et al.,

2019; Wohltmann et al., 2020; Dameris et al., 2021; Grooß and Müller, 2021; von der Gathen et al., 2021; Ardra et al., 2022). Polar ozone depletion is ultimately driven by chlorine and bromine substances released to the atmosphere as a result of human activities. (Although there are also bromine and chlorine substances with natural sources, WMO, 2022). The release of the human made chlorine and bromine substances to the atmosphere has led to a substantial increase in the atmospheric halogen

25 loading in the latter half of the last century; human made halogen compounds started increasing substantially in the atmosphere since the 1960s. Consequently, with the stratospheric halogen loading declining since about 2000, the first signs of recovery of both the Antarctic ozone hole and global ozone levels are observed (e.g., Várai et al., 2015; Kuttippurath and Nair, 2017; Strahan and Douglass, 2018; WMO, 2022; Bodeker and Kremser, 2021; Stone et al., 2021; Weber et al., 2022; Johnson et al., 2023).

30 Chemistry-climate models allow many characteristics of the global total column ozone field to be reproduced, but there is a considerable spread among models in the predictions of the absolute ozone column and the simulation of the Antarctic ozone hole is often not satisfactory. Possible reasons could be deficiencies in the model dynamics or in the stratospheric chemistry scheme of chemistry-climate models (Struthers et al., 2009; Dhomse et al., 2018). Such issues also impact the reliability and the accuracy of projections of the recovery of the Antarctic ozone hole under different climate scenarios for the future including

35 climate intervention (Jöckel et al., 2016; Dhomse et al., 2018; Tilmes et al., 2021).

For polar stratospheric ozone depletion to occur, chlorine (which mostly prevails in the stratosphere in the form of the reservoir species HCl and $ClONO_2$) needs to be converted to an ozone destroying form. That is, HCl and $ClONO_2$ need to be "activated" by heterogeneous reactions on polar stratospheric clouds (PSCs) and cold sulphate aerosol particles (Portmann et al., 1996; Solomon, 1999; Shi et al., 2001; Drdla and Müller, 2012; WMO, 2022; Tritscher et al., 2021). Ozone depletion

40 occurs with the return of sunlight to the polar region; this time period is characterised by maintenance of high levels of active chlorine (e.g., Santee et al., 2005; Santee et al., 2008; Solomon et al., 2015; Nedoluha et al., 2016; Jurkat et al., 2017; Wohltmann et al., 2017; Müller et al., 2018; Johansson et al., 2019). PSCs are present in the Antarctic lower stratosphere throughout winter until early October, whereas in the Arctic PSCs occur with much greater year-to-year variability (Pitts et al., 2009; Spang et al., 2018).

45 In the initial step of chlorine activation, in the heterogeneous reaction

$$HCl + ClONO_2 \rightarrow Cl_2 + HNO_3 \quad\quad\quad\quad\quad\quad (R1)$$

the available $ClONO_2$ is titrated against HCl (e.g., Solomon et al., 1986; Wohltmann et al., 2017). In the Antarctic lower stratosphere, the initial concentrations of HCl are greater than those of $ClONO_2$ (Jaeglé et al., 1997; Santee et al., 2008; Nakajima et al., 2020), so that there is no full activation in this step. Then a period of relatively little chemical change in polar

50 night follows ("sleeping chemistry"). Later, in austral spring, the strongest ozone depletion occurs; during this period high values of active chlorine ($ClO_x = Cl + ClO + 2 \times Cl_2O_2$) are maintained in spite of increasingly rapid formation of HCl in the gas phase (Müller et al., 2018). The maintenance of high ClO_x values during this period is accomplished by effective reaction cycles ("HCl null cycles") in which deactivation (i.e. production of HCl) is immediately balanced by the heterogeneous reaction

of HCl with HOCl

55     $HCl + HOCl \rightarrow Cl_2 + H_2O$.   (R2)

(Crutzen et al., 1992; Prather, 1992). This period of high ClO_x and strong ozone loss in the Antarctic ends with a very rapid formation of HCl leading to a practically complete conversion of ClO_x to HCl (i.e., to deactivation) (e.g., Crutzen et al., 1992; Douglass et al., 1995; Grooß et al., 1997; Grooß et al., 2011; Nakajima et al., 2020). However, very rarely, when the Antarctic vortex is perturbed by a sudden stratospheric warming, significant deactivation into $ClONO_2$ may also occur in Antarctica

60   (Grooß et al., 2005; Smale et al., 2021).

Heterogeneous chlorine activation, enhanced concentrations of active chlorine and subsequent ozone loss occur frequently in the polar regions and – under exceptional circumstances – in the mid-latitudes for conditions of low temperatures and enhanced water vapour. The surfaces for heterogeneous reactions might be provided by stratospheric ice particles, stratospheric sulphate aerosol particles (potentially enhanced by volcanic eruptions or climate intervention) or by wildfire smoke injected

65   into the stratosphere (e.g. Solomon et al., 1997; Tilmes et al., 2008; von Hobe et al., 2011; Klobas et al., 2017; Robrecht et al., 2019, 2021; Tilmes et al., 2021; Ohneiser et al., 2022; Santee et al., 2022).

In the present study, we extend earlier work (Grooß et al., 2011; Müller et al., 2018; Zafar et al., 2018) investigating the chemical processes in the core of the Antarctic vortex, in the lower stratosphere (16–18 km, 85–55 hPa, 390–430 K), where extremely low ozone mixing ratios are reached regularly (Solomon et al., 2005; Johnson et al., 2023). We use now the most

70   recent recommendation (Burkholder et al., 2020) of chemical kinetics and photochemical data. And we focus on the impact of Antarctic dehydration (e.g., Kelly et al., 1989; Vömel et al., 1995; Nedoluha et al., 2002; Jiménez et al., 2006; Ivanova et al., 2008; Rolf et al., 2015). Further, the impact of very low HCl mixing ratios in Antarctic winter (Wohltmann et al., 2017; Grooß et al., 2018) is now considered. Both dehydration and very low HCl mixing ratios are clearly observed in the atmosphere.

Taking into account the observed dehydration in the Antarctic vortex (see also section 2.2.1 below for details) reduces

75   substantially the occurrence of ice clouds in the model. A lower occurrence of ice clouds reduces substantially the uptake of HNO_3 on ice particles.

Assuming an HCl mixing ratio of zero after polar night while keeping total inorganic chlorine (Cl_y) constant (Wohltmann et al., 2017; Grooß et al., 2018, see also section 2.2.2 below for details) approximately takes into account the observed very low HCl mixing ratios in the Antarctic vortex in mid-winter. This assumption leads to very low HCl mixing ratios throughout

80   Antarctic spring.

The simulations presented here show that neither of these two assumptions has a very strong effect on the simulated chemical ozone depletion compared to earlier work (Müller et al., 2018; Zafar et al., 2018); similarly, using the most recent recommendation (Burkholder et al., 2020) has little impact. Severe ozone depletion to values below 50 ppb is simulated (consistent with observations) for the South Pole in late September and early October.

85   In summary, our box-model calculations of Antarctic chlorine and ozone chemistry corroborate earlier findings that HCl null cycles, in the core of the vortex in the lower stratosphere in spring are effective in allowing high levels of active chlorine to be maintained and rapid ozone loss to proceed. The reaction of $CH_3O_2 + ClO$ is important for the HCl null cycle initiated by the

reaction $CH_4 + Cl$. We show here that these conclusions are not changed when current kinetic recommendations (Burkholder et al., 2020) are employed or when dehydration and very low HCl mixing ratios observed in polar winter are taken into account.

2 Methods

2.1 Chemical model

The simulations reported here were performed with the Chemical Lagrangian model of the Stratosphere (CLaMS, McKenna et al., 2002; Grooß et al., 2005, 2018) with a set-up following closely the one used in earlier studies (see Grooß et al., 2011; Müller et al., 2018; Zafar et al., 2018, for details). Briefly, here, the stratospheric chemistry is calculated for particular air parcels along three-dimensional trajectories. To integrate the differential equations representing the set of chemical reactions considered here, we use the solver SVODE (Brown et al., 1989). Chemical rate constants and photolysis cross sections generally are taken from the most current recommendation (Burkholder et al., 2020), but the earlier recommendations by Sander et al. (2011) were used for comparison. Photolysis rates are calculated in spherical geometry (Becker et al., 2000). Heterogeneous chemistry in the model (see Grooß et al., 2011; Müller et al., 2018, for details) is assumed to occur on the surface of ice and nitric acid trihydrate (NAT, with a particle density of $3 \cdot 10^{-3}$ cm^{-3}) as well as in liquid ternary particles ($HNO_3/H_2SO_4/H_2O$) and cold liquid binary (H_2SO_4/H_2O) particles (Burkholder et al., 2020).

2.2 Trajectory and chemical set-up

Here trajectories for the austral winter 2003 are used, which are defined by the location and time of minimum ozone measured by ozone sondes at the South Pole. Forward and backward trajectories are calculated from the South Pole measurements. (Grooß et al., 2011; Müller et al., 2018). We focus on one particular trajectory passing through the location of an ozone sonde measurement at South Pole; 14 ppb O_3 at 74 hPa (391 K) on 24 September 2003 (Grooß et al., 2011). The same trajectory was investigated in earlier work (Müller et al., 2018; Zafar et al., 2018) and is referred to below as the reference trajectory. Meteorological data were taken from operational analyses of the European Centre for Medium-range Weather Forecasts (ECMWF) and diabatic descent rates of the air-parcels were calculated using a radiation code (Zhong and Haigh, 1995) and climatological ozone and water vapour profiles (Grooß and Russell, 2005).

The initial mixing ratios for the reference trajectory for the main trace gases on 1 June are listed in Table 1; with the exception of H_2O they are the same as in earlier work (Müller et al., 2018; Zafar et al., 2018). These initial conditions imply the assumption that for the air parcels in question, the initial step of heterogeneous chlorine activation (reaction R1) has already occurred, so that ClO_x values are enhanced and the HCl mixing ratio is lower than at the beginning of the winter. Further, denitrification is also represented in the initial conditions by assuming $HNO_3 = 4.5$ ppb. The sensitivity of the results of the simulations on the initial ozone and initial HNO_3 mixing ratios, as well as the impact of assumptions on the chemistry of methylhypochlorite (CH_3OCl) and the methyl peroxy radical (CH_3O_2) has been discussed in previous work (Müller et al., 2018; Zafar et al., 2018).

O_3	2.2 ppm
H_2O	2.05 ppm
CH_4	1.2 ppm
HNO_3	4.5 ppb
HCl	1.05 ppb
ClO_x	1.01 ppb
$ClONO_2$	12 ppt
HOCl	4.65 ppt
Br_y	17 ppt
CO	16 ppb

Table 1. Initial mixing ratios (for 1 June) of atmospheric trace gases used for the CLaMS simulation along the reference trajectory.

2.2.1 Initial water vapour

120 There is one important exception to the initial values used previously, namely the initial value of water vapour. Assuming $H_2O = 4.1$ ppm (Müller et al., 2018; Zafar et al., 2018) means essentially that dehydration of the Antarctic stratosphere is neglected. However, every year irreversible dehydration through ice particle sedimentation occurs with the removal of water vapour from the air at sufficiently low (ice-formation) temperatures (e.g., Jiménez et al., 2006; Tritscher et al., 2019, 2021). Particles of different sizes will sediment at different rates (Müller and Peter, 1992). Further, there is a year-to-year variability in

125 the extent and timing of the severity of Antarctic dehydration (e.g., Nedoluha et al., 2002) and the dehydration is not uniform throughout the Antarctic vortex (Kelly et al., 1989; Ivanova et al., 2008). Nonetheless, strong dehydration in the Antarctic winter vortex (in June, July, August) has been reported consistently both for in-situ and remote sensing measurements as well as for model simulations (Kelly et al., 1989; Vömel et al., 1995; Nedoluha et al., 2002; Jiménez et al., 2006; Ivanova et al., 2008; Schoeberl and Dessler, 2011; Rolf et al., 2015; Poshyvailo et al., 2018; Tritscher et al., 2019, 2021).

130 Kelly et al. (1989) report minimum values of H_2O based on aircraft measurements down to 1.5 ppm (at about ≈ 350 K) and H_2O mixing ratios of 2.0-2.4 ppm for an isentropic flight on 430 K on 2 September 1987. Kelly et al. (1989) also report temperatures corresponding to ice saturation mixing ratios of ~ 2 ppm over an altitude range 350-450 K in late August at the South Pole. Vömel et al. (1995) conducted a series of balloon measurements with a frost point hygrometer from McMurdo station (in 1990) and South Pole (1990-1994) and find an average mixing ratio of H_2O of 2.3 ppm between 16 and 18 km.

135 Ivanova et al. (2008) report airborne H_2O measurements in the core of the Antarctic vortex on 21 and 23 September and 2 and 8 October 1999 during the APE-GAIA campaign – measurements at 410-430 K cover the range between 1.8-2.5 ppm mixing ratio of H_2O. Jiménez et al. (2006), based on observations by the Microwave Limb Sounder (MLS) report reductions of H_2O up to ~ 3 ppm – they find H_2O mixing ratios at ~ 17 km (440 K) at about 80°S equivalent latitude on 15 September of 2-2.2 ppm water vapour.

140   Here (for about 430 K) we assume an initial mixing ratio of $H_2O = 2.05$ ppm, which accounts for the observed dehydration in Antarctica; 2.05 ppm of water vapour will remain in the gas-phase if a temperature of ~ 185 K is reached in the atmosphere. A value for initial $H_2O = 2.05$ is also close to the value of initial $H_2O = 2.2$ ppm employed in earlier work (Crutzen et al., 1992).

2.2.2   Initial HCl

145 For Antarctic HCl, a discrepancy between simulations and observations between May and July was reported (Wohltmann et al., 2017; Grooß et al., 2018); during this period model simulations significantly overestimate the observed HCl mixing ratios. The process causing this discrepancy between observations and simulations is not known at this point in time (but it must be a process missing in the models). Different options include an increased uptake of HCl into PSC particles (Wohltmann et al., 2017), a temperature bias of the underlying meteorological analyses, and unknown (possibly heterogeneous) chemical
150 reactions (Grooß et al., 2018).

    Here we do not investigate a process missing in models (Wohltmann et al., 2017; Grooß et al., 2018); rather our choice of the initial conditions is aimed at estimating the maximum possible effect of the very low HCl mixing ratios on HCl null cycles, ClO_x, and ozone depletion. This is the case when assuming initial HCl to be zero, with a corresponding increase in ClO_x, i.e., initial Cl_y is unchanged in the simulations.

155 ### 2.3   Kinetic and photochemical parameters

Simulation	Initial HCl	Initial H_2O	Kinetics (JPL recomm.)	Colour
S1	HCl = 1.05 ppb	H_2O = 4.1 ppm	(Sander et al., 2011)	magenta
S2	HCl = 1.05 ppb	H_2O = 4.1 ppm	(Burkholder et al., 2020)	ochre
S3	HCl = 1.05 ppb	H_2O = 2.05 ppm	(Burkholder et al., 2020)	blue
S4	HCl = 0.0 ppb	H_2O = 2.05 ppm	(Burkholder et al., 2020)	red

Table 2. Employed assumptions for four different box-model simulations (S1-S4) a long the reference trajectory. The colours refer to those used in Figs. 2, 4, and 5 below.

    In the results presented below, the sensitivity of Antarctic chlorine chemistry and ozone loss in spring to dehydration, to low early winter HCl mixing ratios and to different recommendations for kinetic parameters (Sander et al., 2011; Burkholder et al., 2020) is explored. The different model simulations (S1-S4) and the employed assumptions (as well as the colours used in the figures below) are summarised in Table 2.

2.3.1 Recent recommendations of chemical kinetic and photochemical data

Müller et al. (2018) and Zafar et al. (2018) presented results of box-model simulations for the lowermost stratosphere in the core of the Antarctic vortex based on earlier recommendations of chemical kinetic and photochemical data by the Jet Propulsion Laboratory (JPL, Sander et al., 2011, simulation S1 in Table 2). Simulation S1 is shown here to establish a link to earlier work. Otherwise (simulations S2-S4) we use here chemical kinetics and photochemical data from the most recent recommendation (Burkholder et al., 2020).

The observed partitioning of ClO and Cl_2O_2 in the Antarctic stratosphere is well represented when the recommendations by Burkholder et al. (2015) are used (Canty et al., 2016). As the rate constants affecting chlorine chemistry were not changed substantially between the recommendations byBurkholder et al. (2015) and (Burkholder et al., 2020) the polar chlorine chemistry is also well represented by the most recent recommendation. The largest remaining uncertainties in the ozone depletion rate are caused by uncertainties in the kinetic parameters influencing the Cl_2O_2 photolysis rate (Kawa et al., 2009; Canty et al., 2016; Wohltmann et al., 2017).

2.3.2 The rate constant of the reaction $ClO + CH_3O_2$
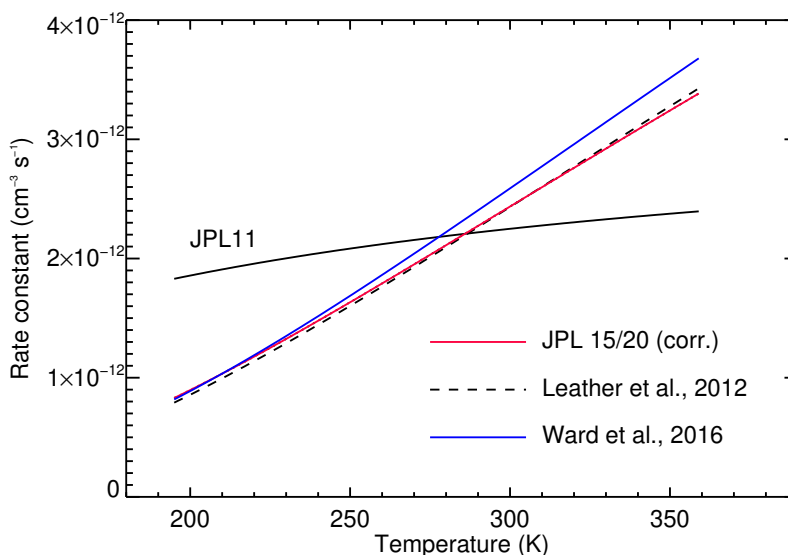
Figure 1. The temperature dependent rate constant for reaction R3 ($ClO + CH_3O3 \longrightarrow$ products) from a variety of sources. The recommendation by Sander et al. (2011) is shown as a black solid line (JPL 11) and the red line (JPL 15/20) is for Burkholder et al. (2015) (and Burkholder et al., 2020) with the corrected value $A = 1.8 \times 10^{-11}$. Also shown are recent measurements (dashed line, Leather et al., 2012); (blue line, Ward and Rowley, 2016).

Compared to the listing in recommendations (Burkholder et al., 2015, 2020) we corrected the rate constant of the reaction

$$ClO + CH_3O_2 \rightarrow prod. \quad ; \quad\quad\quad\quad\quad\quad\quad\quad\quad\quad\quad\quad\quad\quad\quad\quad\quad\quad\quad\quad (R3)$$

175 the *A*-factor for the rate constant of reaction R3 is taken to be

$$A = 1.8 \times 10^{-11} \quad \text{and not} \quad A = 1.8 \times 10^{-12}; \tag{1}$$

the latter value is listed incorrectly (an obvious typo; J. Burkholder, pers. comm.) both in Burkholder et al. (2015) and Burkholder et al. (2020). The temperature dependent rate constant is listed in Sander et al. (2011) as:

$$k_{\text{jpl11}}(T) = 3.3 \times 10^{-12} \cdot \exp\left(-\frac{1}{115} \cdot \frac{1}{T}\right) \tag{2}$$

180 where T is temperature. This recommendation was updated by Burkholder et al. (2015) and Burkholder et al. (2020), but the correct equation is:

$$k_{\text{jpl15/20}}(T) = 1.8 \times 10^{-11} \cdot \exp\left(-\frac{1}{600} \cdot \frac{1}{T}\right) \tag{3}$$

We show the reaction rate constant in equation 3 against the recommendation reported by Sander et al. (2011) and other recent measurements (Leather et al., 2012; Ward and Rowley, 2016) (Fig. 1).

$k(298\,\text{K})$	Source
$2.243 \cdot 10^{-12}$	Sander et al. (2011)
$2.404 \cdot 10^{-12}$	Burkholder et al. (2015, 2020)
$2.399 \cdot 10^{-12}$	Leather et al. (2012)
$2.552 \cdot 10^{-12}$	Ward and Rowley (2016)

Table 3. The rate constant k of reaction R3 ($\text{ClO} + \text{CH}_3\text{O}_2 \longrightarrow$ products) at 298 K. Note that the correct value for the A-factor is: $A = 1.8 \times 10^{-11}$ (which is not listed correctly in recommendations, see eq. 1).

185 Using the incorrect *A*-factor would result in a rate constant $k_{\text{jpl15/20}}$ which is inconsistent with laboratory measurements. Further, when calculating the reaction rate at room temperature $k(298\,\text{K})$, the formulation of equation 3 yields consistent results with earlier work and also reproduces the $k(298\,\text{K})$ value reported in Burkholder et al. (2015, 2020), see Table 3.

A simulation employing the incorrect *A*-factor in the rate constant of reaction R3 leads to underestimating the rate constant for reaction R3 by a factor of ten. Assuming this incorrect value (for R3) in simulation S4 yields a slower HCl increase in early

190 October and the minimum ozone mixing ratio reached is 30.6 ppb instead of 5.7 ppb in simulation S4.

Assuming a too low (by a factor of ten) value for reaction R3 is not equivalent to neglecting reaction R3 completely. Removing reaction R3 completely from the set of reactions considered here leads to a weaker rate of ozone depletion and to a much larger value for minimum ozone (more than 100 ppb), whereas the simulated minimum ozone is $\approx$ 6 ppb, when reaction R3 is taken into account correctly.

195 Further, the temporal development of HCl is very different; when neglecting reaction R3, the increase in HCl is much less steep. Using the value for reaction R3 listed in the recommendations (Burkholder et al., 2015, 2020) shows very low HCl values on 10 September (below 0.1 ppb), whereas HCl on this day is about 0.6 ppb when reaction R3 is neglected. Using the correct value for reaction R3 (eq. 3) results in even lower HCl values (close to zero).

3 Results

3.1 Comparing the chemical kinetic and photochemical recommendations by Sander et al., 2011 and Burkholder et al., 2020

A comparison is shown (Fig. 2) for the box model simulation (S1) based on the kinetic and photochemical recommendations by Sander et al. (2011), (Müller et al., 2018; Zafar et al., 2018, which were used in earlier work) and Burkholder et al. (2020), the most recent recommendation (S2). The results for HCl, ClO_x, HOCl, $ClONO_2$, and O_3 reported earlier (magenta lines in Fig. 2; simulation S1 in Table 2) showed that at 16–18 km (85–55 hPa) in the core of the vortex, high levels of active chlorine are maintained by HCl null cycles, where the formation of HCl is balanced by immediate reactivation (Müller et al., 2018; Zafar et al., 2018). The strongest ozone loss rates occur in September. The results when using the most recent recommendation (Burkholder et al., 2020) are very similar to those reported earlier. However, levels of HCl in September are somewhat lower (and thus ClO_x somewhat higher, resulting in somewhat stronger ozone loss) when using the recommendations by Sander et al. (2011). The maximum difference between the two runs using different kinetic recommendations (Fig. 2) is less than 0.025 ppm (or 25 ppb) although the relative difference is substantial.

3.2 The impact of initial water vapour

In Fig. 4 simulations are compared for a different initialisation of H_2O, namely H_2O = 4.11 ppm (simulation S2) and H_2O = 2.05 ppm (a more realistic initialisation for H_2O, simulation S3); both simulations are employing Burkholder et al. (2020). For an initial water vapour mixing ratio of 2.05 ppm, both the area of ice PSCs and the mixing ratio of gas-phase water vapour are substantially smaller than for an initial water vapour mixing ratio of 4.11 ppm (Fig. 3). In particular, the simulated ice surface for H_2O_{ini} = 2.05 ppm is substantially lower than for H_2O_{ini} = 4.11 ppm.

However, the very different ice surface between the two simulations has remarkably little impact on the temporal development of HCl and active chlorine with consequences for chemical ozone depletion (Fig. 4). This is consistent with the notion that the actual *rate constant* of the heterogeneous reactions (but not the *occurrence* heterogeneous reactions) within HCl null cycles is of little relevance for the efficacy of the HCl null cycles. The rate constant of heterogeneous reactions is influenced strongly by the type of the available PSC particles. The efficacy of the HCl null cycles, however, are limited by the rate of the reaction of Cl with CH_4 and CH_2O (see appendix A). The HCl null cycles are relevant for the maintenance of high levels of active chlorine (Müller et al., 2018).

Further, a substantial difference in initial water vapour mixing ratios does not result in a substantial difference of polar chlorine chemistry and ozone loss (Fig. 4). There is a slightly lower minimum value of ozone ($\approx$ 10 ppb lower) for an initial water vapour mixing ratio of 4.11 ppm. The simulated ozone values for an initial water vapour mixing ratio of 2.05 ppm are very similar to those for an initial water vapour mixing ratio of 4.11 ppm in June and July and are $\approx$ 50 ppb higher between August and mid-September; the largest *difference* ($\approx$ 100 ppb) in ozone mixing ratios is reached in mid to late September.

A significant difference between the runs for a different initial water vapour mixing ratio is a different concentration of gas-phase HNO_3 – caused by the uptake of HNO_3 onto ice particles (Fig. 3, bottom). The enhanced gas-phase HNO_3 (for initial
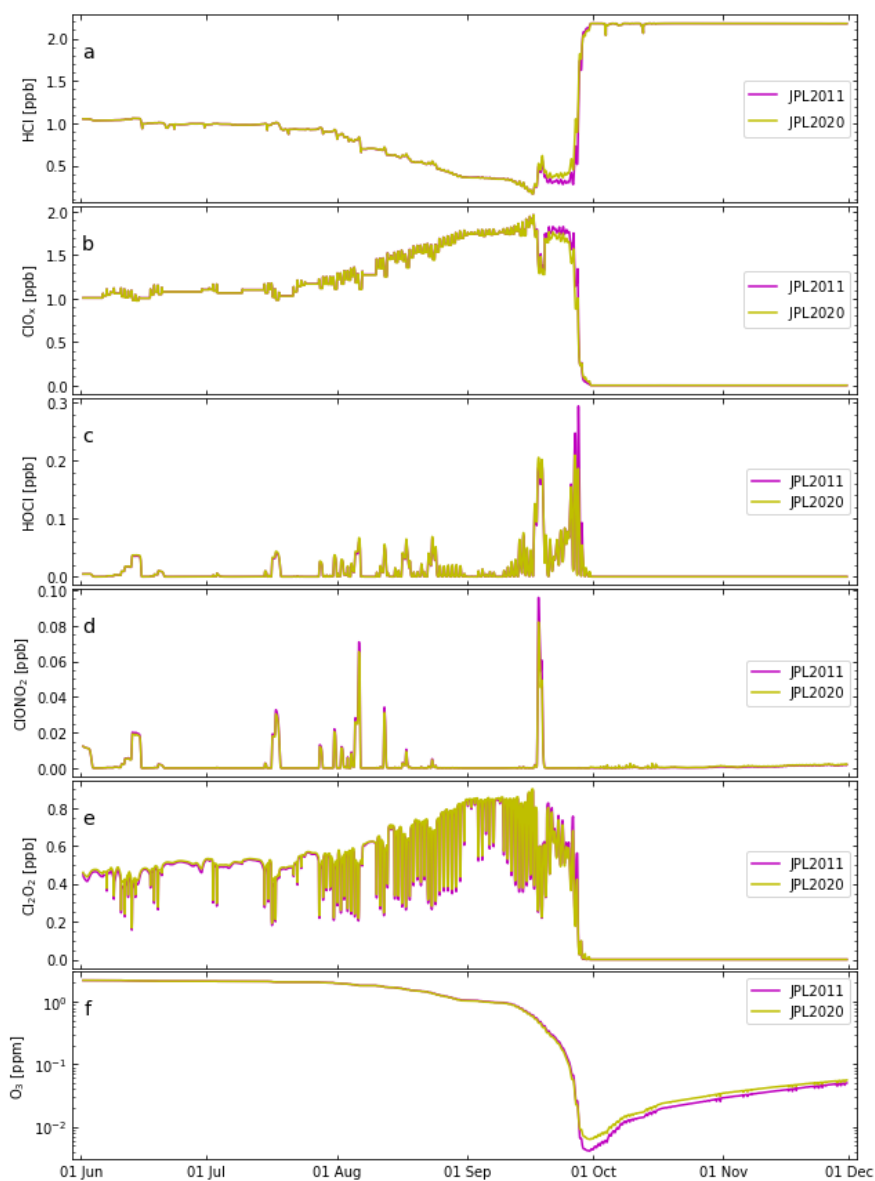
Figure 2. Box-model simulations along a trajectory passing through the location of the ozone sonde observation at South Pole of 14 ppb on 74 hPa (391 K) on 24 September 2003 (Grooß et al., 2011; Müller et al., 2018; Zafar et al., 2018, reference trajectory similar as in earlier studies) using the recommendations from Sander et al. (2011) (simulation S1, magenta lines) and Burkholder et al. (2020) (simulation S2, ochre lines). (See also Table 2). Top panel (a) shows HCl (b) ClO_x, (c) HOCl, (d) $ClONO_2$, (e) Cl_2O_2, and (f) ozone (log-scale). The results for simulation S1 using Sander et al. (2011) are identical to those presented earlier (Müller et al., 2018; Zafar et al., 2018).
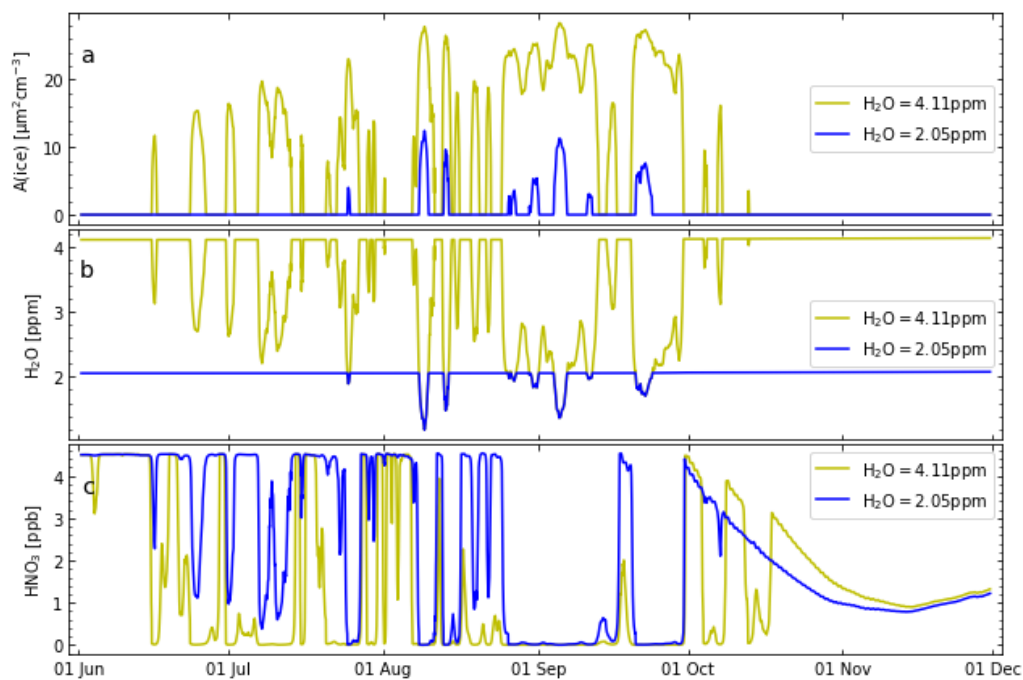
Figure 3. The simulated temporal development of ice surface (top panel, a), gas-phase water vapour concentrations (middle panel, b) and gas-phase HNO_3 concentrations (bottom panel, c). The results for both initial water vapour mixing ratio of 4.11 ppm (simulation S2, ochre lines) and 2.05 ppm (simulation S3, blue lines) are shown. (See also Table 2 for further details).

water vapour mixing ratio of 2.05 ppm) allows more NO_x to be released to the gas phase and (in sun-light) leads to somewhat more formation of $ClONO_2$ (Fig. 4).

3.3 Impact of initial HCl

235   We conducted a simulation (for $H_2O_{initial} = 2.05$ ppm) assuming $HCl_{initial} = 0$ (see Sec. 2.2), which corresponds to an increase in initial active chlorine ($ClO_{x,initial} = 2.26$ ppb); that is we assume Cl_y = const. (Fig. 5). Assuming an initial value of HCl = 0 for early June (red lines in Fig. 5) resembles the conditions in the atmosphere (Wohltmann et al., 2017; Grooß et al., 2018, see also section 2.2 above), while an initial value of HCl = 1.05 ppb (blue lines in Fig. 5) is closer to HCl values in current model simulations.

240   As expected, for more initial ClO_x, there is a somewhat stronger ozone depletion (Fig. 5, bottom panel, red line). The difference in ozone between the two simulations is below $\approx$ 100 ppb in June and July but increases to $\approx$ 400 ppb in September. However, the ozone minimum values reached, differ only by $\approx$ 10 ppb. Overall, the difference in absolute ozone depletion between the two simulations (S3 and S4) is moderate (albeit not in relative terms) in accordance with the conclusions by Grooß et al. (2018).
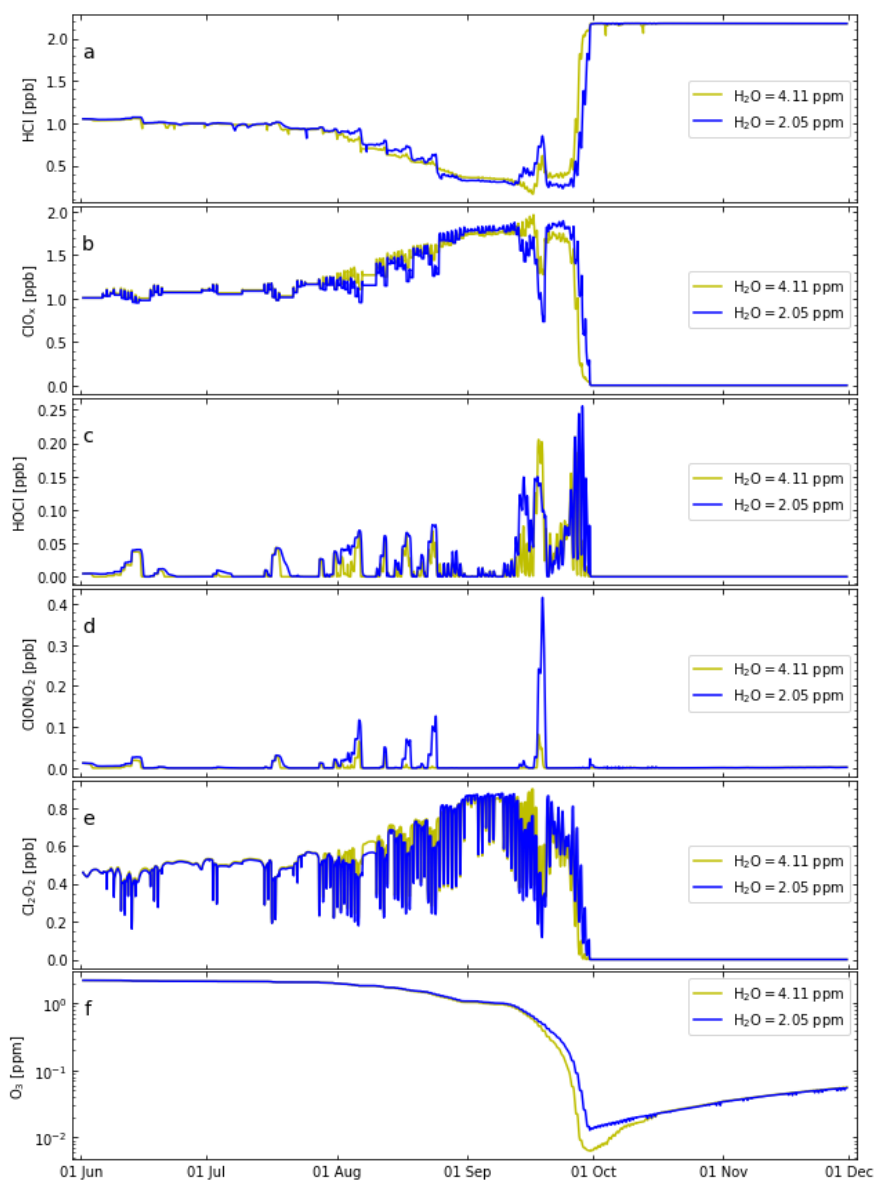
Figure 4. Similar as Fig. 2 but using the recommendations from Burkholder et al. (2020). Results are compared for a different initialisation of H_2O; $H_2O = 4.11$ ppm (simulation S2, ochre lines) and $H_2O = 2.05$ ppm (simulation S3, blue lines). (See also Table 2).
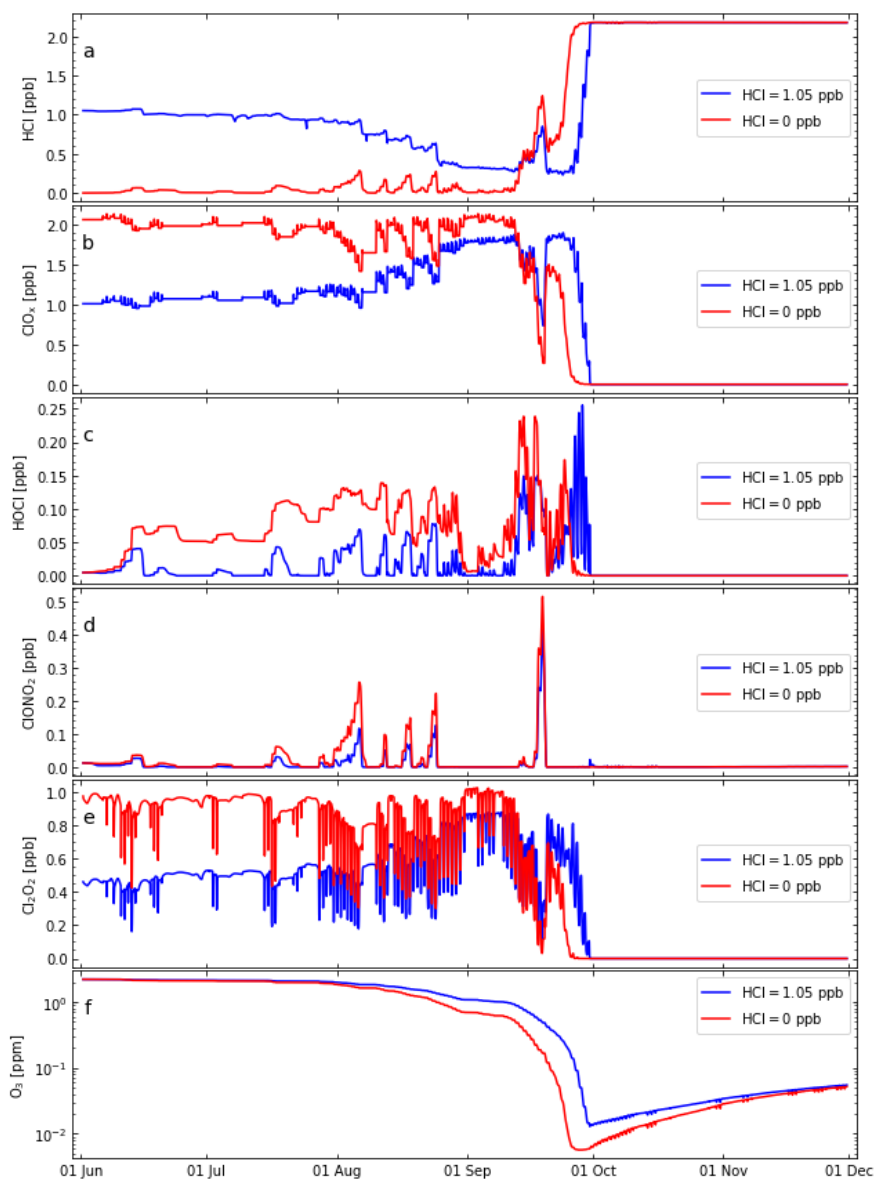
Figure 5. Similar as Fig. 4 (for initial $H_2O = 2.05$ ppm) but comparing the results for simulation S3 (blue lines) with the results for simulation S4 (red lines), where a different initialisation of HCl and active chlorine (ClO_x) was used. The kinetic recommendations of Burkholder et al. (2020) are used. (See also Table 2).
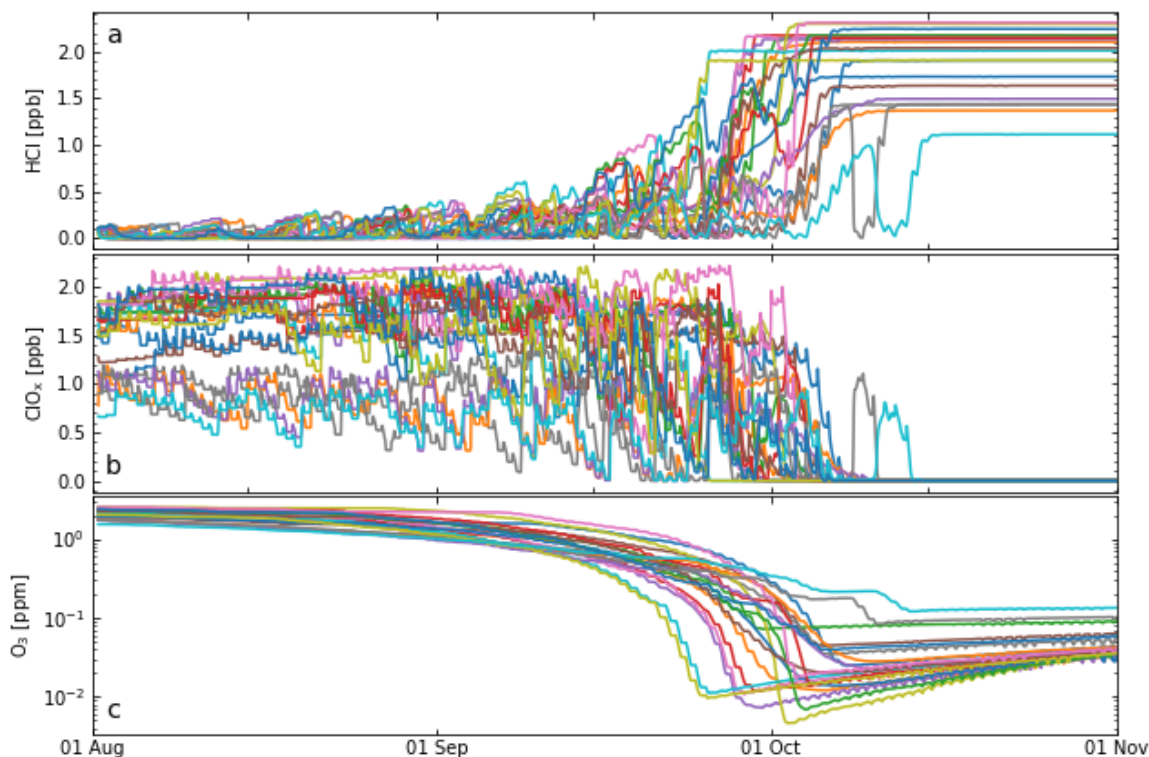
Figure 6. Results from multi-trajectory simulations (21 trajectories) of the CLaMS box-model. The trajectories are consistently initialised (for 1 August) as in Grooß et al. (2011), which corresponds well with the assumptions made for simulation S4 (see text for details). Simulations were performed for a set of trajectories passing the South Pole at 400 K (Grooß et al., 2011). The results of the box-model simulations are shown for the time period from 1 August to 1 November 2003. Panel (a) shows HCl, panel (b) ClO$_x$, and panel (c) ozone. Individual trajectories are shown in different colour to allow them to be distinguished more easily.

245   However, HOCl mixing ratios are substantially higher for HCl$_{initial} = 0$ (in particular from mid-June to mid-August). Further, the HCl mixing ratios remain low from June to mid September indicating that the HCl null cycles are effective in maintaining low HCl mixing ratios (Müller et al., 2018). When ozone mixing ratios reach extremely low values in late September, HCl mixing ratios increase rapidly, which occurs a few days earlier in the case of HCl$_{initial} = 0$ (Fig. 5).

3.4 Multi-trajectory simulations

250 Similar as in earlier work (Grooß et al., 2011; Müller et al., 2018), we selected here twenty one trajectories passing the South Pole (in late September/early October) at the 400 K potential temperature level; these trajectories include diabatic descent and latitude variations. We use the most recent kinetic recommendations (Burkholder et al., 2020). From early August to early October these trajectories show roughly the same diabatic descent of ≈ 10 K, similarly as the reference trajectory discussed

above. However, over this period, the different trajectories show strong variations in latitude (and thus exposure to sunlight);
the latitude varies between the South Pole and $\approx 65°S$ with some equatorward excursions to $\approx 60°S$ and, sometimes to $\approx 55°S$.

The initial values (for 1 August) were taken from Grooß et al. (2011); briefly denitrification and dehydration are taken into account, total chlorine (Cl_y) is deduced from observations (correlation with N_2O) and the HCl initialisation is taken from a climatology based on ACE-FTS (Atmospheric Chemistry Experiment – Fourier Transform Spectrometer) measurements (Jones et al., 2012). Overall, these initial conditions correspond well with the assumptions made for simulation S4. Since the initial value of Cl_y is taken from (Grooß et al., 2011), also the initial ClO_x is different for the individual trajectories.

The results of the multi-trajectory simulations (Fig. 6) show a certain variability in the ozone loss rate, which depends strongly on solar insolation and on the initial value of ClO_x; also note that initial ozone is different for the individual trajectories. The minimum ozone is reached for the individual trajectories between late September and early October. There is also a certain variability of the temporal development of HCl, with some trajectories showing intermittent increases in HCl for certain periods (but no complete deactivation).

However, all trajectories show strongly enhanced values of ClO_x over the period of strong ozone loss in August and September, consistent with suppressed values of HCl (Fig. 6). Minimum ozone values for all trajectories are very low; below ≈ 100 ppb for most and below 10 ppb for several trajectories (Fig. 6). The period of rapid ozone loss (driven by high levels of ClO_x) ends abruptly with chlorine deactivation through very rapid formation of HCl (e.g., Crutzen et al., 1992; Douglass et al., 1995; Grooß et al., 1997; Müller et al., 2018). After deactivation, HCl values remain high and practically unchanged in the box model simulation.

4 Discussion

Simulations of Antarctic chlorine and ozone chemistry for the core of the Antarctic vortex (16–18 km, 85–55 hPa, 390–430 K) indicate that HCl null cycles (C1 and C2, see appendix A) are effective throughout winter and spring (Grooß et al., 2011; Müller et al., 2018). The HCl null cycles require sufficiently low temperatures so that heterogeneous reactions (in particular reaction R2) have significant reaction rates. Further a significant rate of the reaction $CH_3O_2 + ClO$ (reaction R3) is important for the efficacy of the HCl null cycle C1 (as discussed earlier, Crutzen et al., 1992; Zafar et al., 2018). The HCl null cycles allow HCl mixing ratios to be maintained at very low values so that rapid ozone depletion proceeds until the deactivation of ClO_x into HCl.

A low value of water vapour in mid winter is suggested here ($H_2O_{ini} = 2.05$ ppm, see also section 2.2.1) to account for the observed dehydration in the Antarctic vortex (e.g., Kelly et al., 1989; Vömel et al., 1995; Nedoluha et al., 2002). This leads to substantially less formation of ice particles (Fig. 3) and thus to a substantially lower rate of heterogeneous reactions on ice as well as less uptake of HNO_3 from the gas phase compared to earlier work (Müller et al., 2018; Zafar et al., 2018). However, ozone depletion is not strongly affected, consistent with the results of Kirner et al. (2015), who used the chemistry-climate model ECHAM5/MESSy for Atmospheric Chemistry (EMAC) to investigate the impact of different types of PSCs on Antarctic chlorine activation and ozone loss. Kirner et al. (2015) find that heterogeneous chemistry on liquid particles is responsible for

more than 90% of the ozone depletion in Antarctic spring and that heterogeneous chemistry on ice particles causes less than 5
DU of additional column ozone depletion. The conclusion that heterogeneous chlorine chemistry is dominated by reactions on
liquid particles is supported also by other work (e.g., Wegner et al., 2012; Grooß and Müller, 2021; Tritscher et al., 2021).

290   Further, Antarctic winter MLS observations during the period of the onset of chlorine activation (between May and July in
austral winter) and ground-based measurements at Syowa station in early July (Nakajima et al., 2020) indicate that very low
mixing ratios of HCl prevail in the vortex, which are not well reproduced by model simulations (Wohltmann et al., 2017; Grooß
et al., 2018). Possible reasons for these very low mixing rations of HCl are discussed in detail above (section 2.2.2).

Accounting for very low HCl values in mid-winter in the initial values of our simulations (see also section 2.2.2), we find
295 very low HCl mixing ratios throughout winter and spring. This result is consistent with HCl values being maintained at very
low values through the efficacy of the HCl null cycles (C1 and C2, see appendix). Further, while ozone depletion is somewhat
enhanced under these conditions, ozone depletion is not strongly affected (and also the minimum values of Antarctic ozone
reached are similar) consistent with Grooß et al. (2018).

5   Conclusions

300 The results of our simulations corroborate earlier findings that effective HCl null cycles (C1 and C2; see Appendix A) allow
high levels of active chlorine to be maintained in the Antarctic lower stratosphere during the period of strong ozone depletion.
During this period, HCl production rates in the gas-phase are high (and increase with decreasing ozone, Grooß et al., 2011;
Müller et al., 2018).

The sensitivity investigations in the present study show the following. First, using the most recent recommendation for
305 chemical kinetic and photochemical data (Burkholder et al., 2020), does not change the results of the simulations substantially
compared to earlier work (where Sander et al., 2011, was used).

Second, the HCl null cycles require the heterogeneous reaction R2 ($HCl + HOCl \rightarrow Cl_2 + H_2O$) to proceed at a substan-
tial rate. Further, the gas-phase reaction R3 ($ClO + CH_3O_2 \rightarrow$ prod.) is essential (for the null cycle initiated by the reaction
$CH_4 + Cl$, see also appendix A and section 2.3.2). If reaction R3 were neglected, HCl mixing ratios in early September of 0.6
310 ppb are simulated, instead of HCl values close to zero. Further simulated minimum ozone is more than 100 ppb instead of ≈ 6
ppb with reaction R3.

Third, taking into account the observed dehydration in the Antarctic lower stratosphere in winter (see section 2.2), which
was neglected in earlier work (Müller et al., 2018; Zafar et al., 2018), substantially reduces the occurrence of ice clouds in the
model but does not affect strongly the results of chlorine chemistry and ozone loss. The most important impact of the simulated
315 difference in the occurrence of ice clouds in the model is caused by the uptake of HNO_3 from the gas-phase into ice particles.
The HNO_3 uptake is smaller, when less ice particle surface is available. If the observed dehydration is taken into account in the
simulations, a slightly higher minimum value of ozone (≈ 10 ppb higher) is simulated.

Finally, the maximum impact of the observed (but unexplained) observation of extremely low values of HCl during polar
night (Wohltmann et al., 2017; Grooß et al., 2018) was investigated based on the current simulations. This is done by assuming

320 an HCl mixing ratio of zero after polar night on 1 June (while keeping Cl_y constant). These assumptions lead to a temporal development of the chlorine chemistry that is different than when assuming a higher initial HCl; in particular HOCl mixing ratios are enhanced from about mid-June to mid-August. Further, ClO_x is enhanced throughout winter and spring, and HCl mixing ratios remain very low until rapid chlorine deactivation occurs into HCl. However the overall ozone depletion in the Antarctic lower stratosphere is not strongly affected (consistent with Grooß et al., 2018); the simulated ozone minimum values

325 differ by $\approx$ 10 ppb. Overall, our simulations indicate extremely low minimum ozone values at the South Pole (below 50 ppb) in late September/early October in agreement with observations (Solomon et al., 2005; Grooß et al., 2011; Johnson et al., 2023).

Code availability. The CLaMS model is accessible via https://jugit.fz-juelich.de/clams/CLaMS (CLaMS, 2022).

Data availability. The model results presented here are attached to the paper as an electronic supplement (in netcdf format).

Appendix A: HCl null cycles

The HCl null cycles listed below are responsible for the maintenance of high levels of active chlorine throughout Antarctic spring and were reported earlier (Müller et al., 2018; Zafar et al., 2018); they are repeated here for reference. Cycle C1 (Crutzen et al., 1992; Müller et al., 2018) starts with HCl production in the reaction $CH_4 + Cl$

$$CH_4 + Cl \quad \rightarrow HCl + CH_3 \tag{AR1}$$
$$CH_3 + O_2 + M \quad \rightarrow CH_3O_2 + M \tag{AR2}$$
$$CH_3O_2 + ClO \quad \rightarrow CH_3O + Cl + O_2 \tag{AR3}$$
$$CH_3O + O_2 \quad \rightarrow HO_2 + CH_2O \tag{AR4}$$
$$ClO + HO_2 \quad \rightarrow HOCl + O_2 \tag{AR5}$$
$$HOCl + HCl \quad \rightarrow Cl_2 + H_2O \tag{AR6}$$
$$Cl_2 + h\nu \quad \rightarrow 2\,Cl \tag{AR7}$$
$$Cl + O_3 \quad \rightarrow ClO + O_2 \quad (2\times) \tag{AR8}$$
$$Net(C1): \quad CH_4 + 2\,O_3 \quad \rightarrow CH_2O + H_2O + 2\,O_2$$
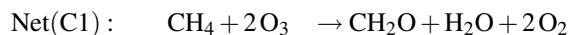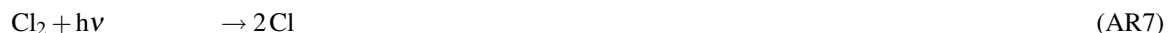
330   Further, the formation of HCl in the reaction

$$CH_2O + Cl \rightarrow HCl + CHO \tag{AR9}$$

leads to the following cycle (C2, Müller et al., 2018):

$$CH_2O + Cl \quad \rightarrow HCl + CHO \tag{AR10}$$
$$CHO + O_2 \quad \rightarrow CO + HO_2 \tag{AR11}$$
$$ClO + HO_2 \quad \rightarrow HOCl + O_2 \tag{AR12}$$
$$HOCl + HCl \quad \rightarrow Cl_2 + H_2O \tag{AR13}$$
$$Cl_2 + h\nu \quad \rightarrow 2\,Cl \tag{AR14}$$
$$Cl + O_3 \quad \rightarrow ClO + O_2 \tag{AR15}$$
$$Net(C2): \quad CH_2O + O_3 \quad \rightarrow CO + H_2O + O_2$$
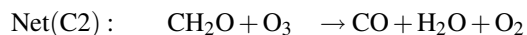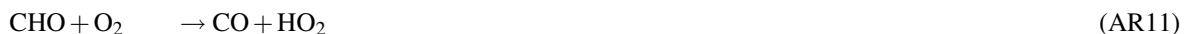
Appendix B: Changes in JPL2015 and JPL2020

In Burkholder et al. (2020) a new algorithm for the formulation of termolecular reactions (association dissociation) was introduced, which is used here. Note the correction (compared to the values listed in the recommendations) to the reaction
335    $ClO + CH_3O_2 \rightarrow$ prod. discussed in detail in section 2.3.

$$
\begin{array}{lcl}
Cl + CH_4 & \rightarrow & HCl + CH_3 \\
ClO + CH_3O_2 & \rightarrow & prod. \\
CFC12 + O(^1D) & \rightarrow & prod. \\
HCFC22 + O(^1D) & \rightarrow & prod. \\
CFC113 + O(^1D) & \rightarrow & prod. \\
HCFC22 + OH & \rightarrow & prod. \\
CH_3Cl + OH & \rightarrow & prod. \\
HO_2 + NO_2 & \rightarrow & HO_2NO_2 \\
HO_2NO_2 & \rightarrow & HO_2 + NO_2 \\
NO_2 + NO_3 & \rightarrow & N_2O_5 \\
ClO + ClO & \rightarrow & Cl_2O_2 \\
Cl_2O_2 & \rightarrow & ClO + ClO \\
BrO + NO_2 & \rightarrow & BrONO_2 \\
OH + CO & \rightarrow & CO_2 + H \\
CH_2O + h\nu & \rightarrow & prod.
\end{array}
$$
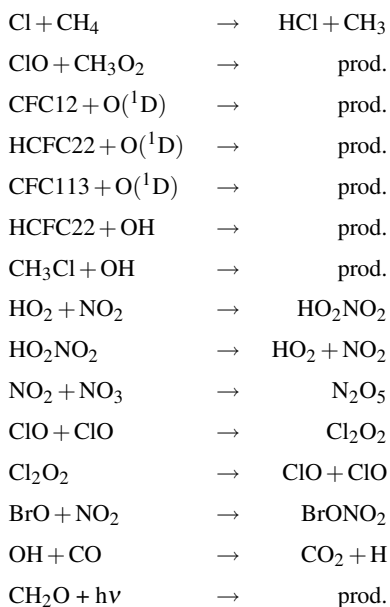
Table A1. Changes between recent recommendations; Sander et al. (2011) versus Burkholder et al. (2015).

$$
\begin{array}{lcl}
CO + OH & \rightarrow & CO_2 + H \\
O(^3P) + NO_2 & \rightarrow & NO + O_2 \\
HO_2 + HO_2 & \rightarrow & H_2O_2 + O_2 \\
HNO_3 + OH & \rightarrow & NO_3 + H_2O \\
HO_2 + NO & \rightarrow & NO_2 + OH \\
NO + NO_3 & \rightarrow & NO_2 + NO_2 \\
H + O_2 & \rightarrow & HO_2 \\
CH_3O_2NO_2 + h\nu & \rightarrow & CH_3O_2 + NO_2
\end{array}
$$
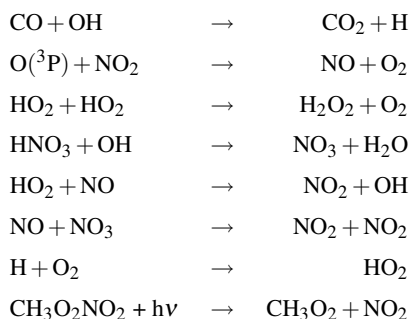
Table A2. Changes between recent recommendations; Burkholder et al. (2015) versus Burkholder et al. (2020).

Author contributions. Y.Z.-L., J.-U.G., and A.M.Z. conducted the simulations with the CLaMS box model that are reported here. R.M. and J.-U.G. conceived and designed the research project. The issues regarding the rate constant of the reaction ClO + CH$_3$O$_2$ (as discussed in section 2.3) were first raised by R.L.. All co-authors discussed the results and contributed to formulating the manuscript.

Competing interests. J.-U.G. and R.M. are editors of ACP; otherwise the authors declare that they have no competing interests

340   *Acknowledgements.*   This paper originates from the Master's thesis of Y. Z-L.; we thank Prof. E. Rühl from the Free University of Berlin for supervising this thesis work. We also thank J. Burkholder for very helpful comments on the rate constant of reaction R3. We thank the European Centre for Medium-range Weather Forecasts (ECMWF) for providing meteorological data sets. This research was partly funded by the "Pilot Lab Exascale Earth System Modelling" project of the Helmholtz association.

References

345 Ardra, D., Kuttippurath, J., Roy, R., Kumar, P., Raj, S., Müller, R., and Feng, W.: The unprecedented ozone loss in the Arctic winter and spring of 2010/2011 and 2019/2020, ACS Earth and Space Chemistry, sp-2021-003338, https://doi.org/10.1021/acsearthspacechem.1c00333, 2022.

Becker, G., Grooß, J.-U., McKenna, D. S., and Müller, R.: Stratospheric photolysis frequencies: Impact of an improved numerical solution of the radiative transfer equation, J. Atmos. Chem., 37, 217–229, https://doi.org/10.1023/A:1006468926530, 2000.

350 Bodeker, G. E. and Kremser, S.: Indicators of Antarctic ozone depletion: 1979 to 2019, Atmos. Chem. Phys., 21, 5289–5300, https://doi.org/10.5194/acp-21-5289-2021, 2021.

Brown, P. N., Byrne, G. D., and Hindmarsh, A. C.: VODE: A variable coefficient ODE solver, SIAM J. Sci. Stat. Comput., 10, 1038–1051, 1989.

Burkholder, J. B., Sander, S. P., Abbatt, J. P. D., Barker, J. R., Huie, R. E., Kolb, C. E., Kurylo, M. J., Orkin, V. L., Wilmouth, D. M., and
355 Wine, P. H.: Chemical kinetics and photochemical data for use in atmospheric studies, Evaluation Number 18, JPL Publication 15-10, 2015.

Burkholder, J. B., Sander, S. P., Abbatt, J. P. D., Barker, J. R., Cappa, C., Crounse, J. D., Dibble, T. S., Huie, R. E., Kolb, C. E., Kurylo, M. J., Orkin, V. L., Percical, C. J., Wilmouth, D. M., and Wine, P. H.: Chemical kinetics and photochemical data for use in atmospheric studies, Evaluation Number 19, JPL Publication 19-5, http://jpldataeval.jpl.nasa.gov, 2020.

360 Canty, T. P., Salawitch, R. J., and Wilmouth, D. M.: The kinetics of the ClOOCl catalytic cycle, J. Geophys. Res., 121, 13 768–13 783, https://doi.org/10.1002/2016JD025710, 2016.

Crutzen, P. J., Müller, R., Brühl, C., and Peter, T.: On the potential importance of the gas phase reaction $CH_3O_2 + ClO \rightarrow ClOO + CH_3O$ and the heterogeneous reaction $HOCl + HCl \rightarrow H_2O + Cl_2$ in "ozone hole" chemistry, Geophys. Res. Lett., 19, 1113–1116, https://doi.org/10.1029/92GL01172, 1992.

365 Dameris, M., Loyola, D. G., Nützel, M., Coldewey-Egbers, M., Lerot, C., Romahn, F., and van Roozendael, M.: Record low ozone values over the Arctic in boreal spring 2020, Atmos. Chem. Phys., 21, 617–633, https://doi.org/10.5194/acp-21-617-2021, 2021.

Dhomse, S. S., Kinnison, D., Chipperfield, M. P., Salawitch, R. J., Cionni, I., Hegglin, M. I., Abraham, N. L., Akiyoshi, H., Archibald, A. T., Bednarz, E. M., Bekki, S., Braesicke, P., Butchart, N., Dameris, M., Deushi, M., Frith, S., Hardiman, S. C., Hassler, B., Horowitz, L. W., Hu, R.-M., Jöckel, P., Josse, B., Kirner, O., Kremser, S., Langematz, U., Lewis, J., Marchand, M., Lin, M., Mancini, E., Marécal, V.,
370 Michou, M., Morgenstern, O., O'Connor, F. M., Oman, L., Pitari, G., Plummer, D. A., Pyle, J. A., Revell, L. E., Rozanov, E., Schofield, R., Stenke, A., Stone, K., Sudo, K., Tilmes, S., Visioni, D., Yamashita, Y., and Zeng, G.: Estimates of ozone return dates from Chemistry-Climate Model Initiative simulations, Atmos. Chem. Phys., 18, 8409–8438, https://doi.org/10.5194/acp-18-8409-2018, 2018.

Douglass, A. R., Schoeberl, M. R., Stolarski, R. S., Waters, J. W., Russell III, J. M., Roche, A. E., and Massie, S. T.: Interhemispheric differences in springtime production of HCl and $ClONO_2$ in the polar vortices, J. Geophys. Res., 100, 13 967–13 978,
375 https://doi.org/10.1029/95JD00698, 1995.

Drdla, K. and Müller, R.: Temperature thresholds for chlorine activation and ozone loss in the polar stratosphere, Ann. Geophys., 30, 1055–1073, https://doi.org/10.5194/angeo-30-1055-2012, 2012.

Grooß, J.-U. and Müller, R.: Simulation of record Arctic stratospheric ozone depletion in 2020, J. Geophys. Res., 126, e2020JD033339, https://doi.org/10.1029/2020JD033339, 2021.

380 Grooß, J.-U. and Russell, J. M.: Technical note: A stratospheric climatology for O$_3$, H$_2$O, CH$_4$, NO$_x$, HCl, and HF derived from HALOE measurements, Atmos. Chem. Phys., 5, 2797–2807, https://doi.org/10.5194/acp-5-2797-2005, 2005.

Grooß, J.-U., Pierce, R. B., Crutzen, P. J., Grose, W. L., and Russell III, J. M.: Re-formation of chlorine reservoirs in southern hemisphere polar spring, J. Geophys. Res., 102, 13 141–13 152, https://doi.org/10.1029/96JD03505, 1997.

Grooß, J.-U., Günther, G., Müller, R., Konopka, P., Bausch, S., Schlager, H., Voigt, C., Volk, C. M., and Toon, G. C.: Simulation of denitrifi-
385   cation and ozone loss for the Arctic winter 2002/2003, Atmos. Chem. Phys., 5, 1437–1448, 2005.

Grooß, J.-U., Konopka, P., and Müller, R.: Ozone chemistry during the 2002 Antarctic vortex split, J. Atmos. Sci., 62, 860–870, 2005.

Grooß, J.-U., Brautzsch, K., Pommrich, R., Solomon, S., and Müller, R.: Stratospheric ozone chemistry in the Antarctic: What controls the lowest values that can be reached and their recovery?, Atmos. Chem. Phys., 11, 12 217–12 226, https://doi.org/10.5194/acp-11-12217-2011, 2011.

390 Grooß, J.-U., Müller, R., Spang, R., Tritscher, I., Wegner, T., Chipperfield, M. P., Feng, W., Kinnison, D. E., and Madronich, S.: On the dis-
       crepancy of HCl processing in the core of the wintertime polar vortices, Atmos. Chem. Phys., pp. 8647–8666, https://doi.org/10.5194/acp-18-8647-2018, 2018.

Ivanova, E. V., Volk, C. M., Riediger, O., Klein, H., Sitnikov, N. M., Ulanovskii, A. E., Yushkov, V. A., Ravegnani, F., Möbius, T., and Schmidt, U.: A quasi-Lagrangian coordinate system based on high resolution tracer observations: implementation for the Antarctic polar
395   vortex, Atmos. Chem. Phys. Discuss., 8, 16 123–16 173, https://doi.org/10.5194/acpd-8-16123-2008, 2008.

Jaeglé, L., Webster, C. R., May, R. D., Scott, D. C., Stimpfle, R. M., Kohn, D. W., Wennberg, P. O., Hanisco, T. F., Cohen, R. C., Proffitt, M. H., Kelly, K. K., Elkins, J., Baumgardner, D., Dye, J. E., Wilson, J. C., Pueschel, R. F., Chan, K. R., Salawitch, R. J., Tuck, A. F., Hovde, S. J., and Yung, Y. L.: Evolution and stoichiometry of heterogeneous processing in the Antarctic stratosphere,, J. Geophys. Res., 102, 13 235–13 253, https://doi.org/10.1029/97JD00935, 1997.

400 Jiménez, C., Pumphrey, H. C., MacKenzie, I. A., Manney, G. L., Santee, M. L., Schwartz, M. J., Harwood, R. S., and Waters, J. W.: EOS MLS observations of dehydration in the 2004–2005 polar winters, Geophys. Res. Lett., 33, L16806, https://doi.org/10.1029/2006GL025926, 2006.

Jöckel, P., Tost, H., Pozzer, A., Kunze, M., Kirner, O., Brenninkmeijer, C., Brinkop, S., Duy, S. C., Dyroff, C., Eckstein, J., Frank, F., Garny, H., Gottschaldt, K.-D., Graf, P., Grewe, V., Kerkweg, A., Kern, B., Matthes, S., Mertens, A., Meul, S., Neumaier, M., Nützel, M.,
405   Oberländer-Hayn, S., Ruhnke, R., Runde, T., Sander, R., Scharffe, D., and Zahn, A.: Earth System integrated Modelling (ESCiMo) with the Modular Earth Submodel System (MESSy) version 2.51, Geosci. Model Dev., 9, 1153–1200, 2016.

Johansson, S., Santee, M. L., Grooß, J.-U., Höpfner, M., Braun, M., Friedl-Vallon, F., Khosrawi, F., Kirner, O., Kretschmer, E., Oelhaf, H., Orphal, J., Sinnhuber, B.-M., Tritscher, I., Ungermann, J., Walker, K. A., and Woiwode, W.: Unusual chlorine partitioning in the 2015/16 Arctic winter lowermost stratosphere: observations and simulations, Atmos. Chem. Phys., 19, 8311–8338, https://doi.org/10.5194/acp-19-
410   8311-2019, 2019.

Johnson, B. J., Cullis, P., Booth, J., Petropavlovskikh, I., McConville, G., Hassler, B., Morris, G. A., Sterling, C., and Oltmans, S.: South Pole Station ozonesondes: variability and trends in the springtime Antarctic ozone hole 1986–2021, Atmos. Chem. Phys., 23, 3133–3146, https://doi.org/10.5194/acp-23-3133-2023, 2023.

Jones, A., Walker, K. A., Jin, J. J., Taylor, J. R., Boone, C. D., Bernath, P. F., Brohede, S., Manney, G. L., McLeod, S., Hughes, R., and Daffer,
415   W. H.: Technical Note: A trace gas climatology derived from the Atmospheric Chemistry Experiment Fourier Transform Spectrometer (ACE-FTS) data set, Atmos. Chem. Phys., 12, 5207–5220, https://doi.org/10.5194/acp-12-5207-2012, 2012.

Jones, A. E. and Shanklin, J. D.: Continued decline of total ozone over Halley, Antarctica, since 1985, Nature, 376, 409–411, https://doi.org/10.1038/376409a0, 1995.

Jurkat, T., Voigt, C., Kaufmann, S., Grooss, J. U., Ziereis, H., Doernbrack, A., Hoor, P., Bozem, H., Engel, A., Boenisch, H., Keber, T., Hueneke, T., Pfeilsticker, K., Zahn, A., Walker, K. A., Boone, C. D., Bernath, P. F., and Schlager, H.: Depletion of ozone and reservoir species of chlorine and nitrogen oxide in the lower Antarctic polar vortex measured from aircraft, Geophys. Res. Lett., 44, 6440–6449, https://doi.org/10.1002/2017GL073270, 2017.

Kawa, S. R., Stolarski, R. S., Newman, P. A., Douglass, A. R., Rex, M., Hofmann, D. J., Santee, M. L., and Frieler, K.: Sensitivity of polar stratospheric ozone loss to uncertainties in chemical reaction kinetics, Atmos. Chem. Phys., 9, 8651–8660, https://doi.org/10.5194/acp-9-8651-2009, 2009.

Kelly, K. K., Tuck, A. F., Murphy, D. M., Proffitt, M. H., Fahey, D. W., Jones, R. L., McKenna, D. S., Loewenstein, M., Podolske, J. R., Strahan, S. E., Ferry and K. R. Chan and J. F. Vedder, G. V., Gregory, G. L., Hypes, W. D., McCormick, M. P., Browell, E. V., and Heidt, L. E.: Dehydration in the lower Antarctic stratosphere during late winter and early spring, 1987, J. Geophys. Res., 94, 11 317–11 357, 1989.

Kirner, O., Müller, R., Ruhnke, R., and Fischer, H.: Contribution of liquid, NAT and ice particles to chlorine activation and ozone depletion in Antarctic winter and spring, Atmos. Chem. Phys., 15, 2019–2030, https://doi.org/10.5194/acp-15-2019-2015, 2015.

Klekociuk, A., Tully, M., Krummel, P., Henderson, S., Smale, D., Querel, R., Nichol, S., and Alexander, S.: The Antarctic Ozone Hole during 2020, Journal of Southern Hemisphere Earth System Science, 72, https://doi.org/doi:10.1071/ES21015, 2022.

Klobas, E. J., Wilmouth, D. M., Weisenstein, D. K., Anderson, J. G., and Salawitch, R. J.: Ozone depletion following future volcanic eruptions, Geophys. Res. Lett., 44, 7490–7499, https://doi.org/https://doi.org/10.1002/2017GL073972, 2017.

Kuttippurath, J. and Nair, P. J.: The signs of Antarctic ozone hole recovery, Sci. Rep., 7, 585, https://doi.org/10.1038/s41598-017-00722-7, 2017.

Leather, K. E., Bacak, A., Wamsley, R., Archibald, A. T., Husk, A., Shallcross, D. E., and Percival, C. J.: Temperature and pressure dependence of the rate coefficient for the reaction between ClO and CH_3O_2 in the gas-phase, Phys. Chem. Chem. Phys., 14, 3425–3434, https://doi.org/10.1039/C2CP22834C, 2012.

McKenna, D. S., Grooß, J.-U., Günther, G., Konopka, P., Müller, R., Carver, G., and Sasano, Y.: A new Chemical Lagrangian Model of the Stratosphere (CLaMS): 2. Formulation of chemistry scheme and initialization, J. Geophys. Res., 107, 4256, https://doi.org/10.1029/2000JD000113, 2002.

Müller, R. and Peter, T.: The numerical modelling of the sedimentation of polar stratospheric cloud particles, Ber. Bunsenges. Phys. Chem., 96, 353–361, 1992.

Müller, R., Grooß, J.-U., Lemmen, C., Heinze, D., Dameris, M., and Bodeker, G.: Simple measures of ozone depletion in the polar stratosphere, Atmos. Chem. Phys., 8, 251–264, https://doi.org/10.5194/acp-8-251-200, 2008.

Müller, R., Grooß, J.-U., Zafar, A. M., Robrecht, S., and Lehmann, R.: The maintenance of elevated active chlorine levels in the Antarctic lower stratosphere through HCl null cycles, Atmos. Chem. Phys., 18, 2985–2997, https://doi.org/10.5194/acp-18-2985-2018, 2018.

Nakajima, H., Murata, I., Nagahama, Y., Akiyoshi, H., Saeki, K., Kinase, T., Takeda, M., Tomikawa, Y., Dupuy, E., and Jones, N. B.: Chlorine partitioning near the polar vortex edge observed with ground-based FTIR and satellites at Syowa Station, Antarctica, in 2007 and 2011, Atmos. Chem. Phys., 20, 1043–1074, https://doi.org/10.5194/acp-20-1043-2020, 2020.

Nedoluha, G. E., Bevilacqua, R. M., and Hoppel, K. W.: POAM III measurements of dehydration in the Antarctic and comparison with the Arctic, J. Geophys. Res., 107, 2002.

455   Nedoluha, G. E., Connor, B. J., Mooney, T., Barrett, J. W., Parrish, A., Gomez, R. M., Boyd, I., Allen, D. R., Kotkamp, M., Kremser, S., Deshler, T., Newman, P., and Santee, M. L.: 20 years of ClO measurements in the Antarctic lower stratosphere, Atmos. Chem. Phys., 16, 10 725–10 734, https://doi.org/10.5194/acp-16-10725-2016, 2016.

Ohneiser, K., Ansmann, A., Kaifler, B., Chudnovsky, A., Barja, B., Knopf, D. A., Kaifler, N., Baars, H., Seifert, P., Villanueva, D., Jimenez, C., Radenz, M., Engelmann, R., Veselovskii, I., and Zamorano, F.: Australian wildfire smoke in the stratosphere: the decay phase in
460   2020/2021 and impact on ozone depletion, Atmos. Chem. Phys., 22, 7417–7442, https://doi.org/10.5194/acp-22-7417-2022, 2022.

Pitts, M. C., Poole, L. R., and Thomason, L. W.: CALIPSO polar stratospheric cloud observations: second-generation detection algorithm and composition discrimination, Atmos. Chem. Phys., 9, 7577–7589, 2009.

Portmann, R. W., Solomon, S., Garcia, R. R., Thomason, L. W., Poole, L. R., and McCormick, M. P.: Role of aerosol variations in anthropogenic ozone depletion in the polar regions, J. Geophys. Res., 101, 22 991–23 006, 1996.

465   Poshyvailo, L., Müller, R., Konopka, P., Günther, G., Riese, M., Podglajen, A., and Ploeger, F.: Sensitivities of modelled water vapour in the lower stratosphere: temperature uncertainty, effects of horizontal transport and small-scale mixing, Atmos. Chem. Phys., 18, 8505–8527, https://doi.org/10.5194/acp-18-8505-2018, 2018.

Prather, M. J.: More rapid ozone depletion through the reaction of HOCl with HCl on polar stratospheric clouds, Nature, 355, 534–537, 1992.

470   Robrecht, S., Vogel, B., Grooß, J.-U., Rosenlof, K., Thornberry, T., Rollins, A., Krämer, M., Christensen, L., and Müller, R.: Mechanism of ozone loss under enhanced water vapour conditions in the mid-latitude lower stratosphere in summer, Atmos. Chem. Phys., 19, 5805–5833, https://doi.org/10.5194/acp-19-5805-2019, 2019.

Robrecht, S., Vogel, B., Tilmes, S., and Müller, R.: Potential of future stratospheric ozone loss in the midlatitudes under global warming and sulfate geoengineering, Atmos. Chem. Phys., 21, 2427–2455, https://doi.org/10.5194/acp-21-2427-2021, 2021.

475   Rolf, C., Afchine, A., Bozem, H., Buchholz, B., Ebert, V., Guggenmoser, T., Hoor, P., Konopka, P., Kretschmer, E., Müller, S., Schlager, H., Spelten, N., Sumińska-Ebersoldt, O., Ungermann, J., Zahn, A., and Krämer, M.: Transport of Antarctic stratospheric strongly dehydrated air into the troposphere observed during the HALO-ESMVal campaign 2012, Atmos. Chem. Phys., 15, 9143–9158, https://doi.org/10.5194/acp-15-9143-2015, 2015.

Sander, S. P., Friedl, R. R., Barker, J. R., Golden, D. M., Kurylo, M. J., Wine, P. H., Abbatt, J. P. D., Burkholder, J. B., Kolb, C. E., Moortgat,
480   G. K., Huie, R. E., and Orkin, V. L.: Chemical kinetics and photochemical data for use in atmospheric studies, JPL Publication 10-6, 2011.

Santee, M. L., Manney, G. L., Livesey, N. J., Foidevaux, L., MacKenzie, I. A., Pumphrey, H. C., Read, W. G., Schwartz, M. J., Waters, J. W., and Harwood, R. S.: Polar processing and development of the 2004 Antarctic ozone hole: First results from MLS on Aura, Geophys. Res. Lett., 32, L12817, https://doi.org/10.1029/2005GL022582, 2005.

Santee, M. L., MacKenzie, I. A., Manney, G. L., Chipperfield, M. P., Bernath, P. F., Walker, K. A., Boone, C. D., Froidevaux, L., Livesey,
485   N. J., and Waters, J. W.: A study of stratospheric chlorine partitioning based on new satellite measurements and modeling, J. Geophys. Res., 113, D12307, https://doi.org/10.1029/2007JD009057, 2008.

Santee, M. L., Lambert, A., Manney, G. L., Livesey, N. J., Froidevaux, L., Neu, J. L., Schwartz, M. J., Millán, L. F., Werner, F., Read, W. G., Park, M., Fuller, R. A., and Ward, B. M.: Prolonged and Pervasive Perturbations in the Composition of the Southern Hemisphere Midlatitude Lower Stratosphere From the Australian New Year's Fires, Geophys. Res. Lett., 49, e2021GL096270,
490   https://doi.org/https://doi.org/10.1029/2021GL096270, e2021GL096270 2021GL096270, 2022.

Schoeberl, M. R. and Dessler, A. E.: Dehydration of the stratosphere, Atmos. Chem. Phys., 11, 8433–8446, https://doi.org/10.5194/acp-11-8433-2011, 2011.

Shi, Q., Jayne, J. T., Kolb, C. E., Worsnop, D. R., and Davidovits, P.: Kinetic model for reaction of ClONO$_2$ with H$_2$O and HCl and HOCl with HCl in sulfuric acid solutions, J. Geophys. Res., 106, 24 259–24 274, https://doi.org/10.1029/2000JD000181, 2001.

495   Smale, D., Strahan, S. E., Querel, R., Frieß, U., Nedoluha, G. E., Nichol, S. E., Robinson, J., Boyd, I., Kotkamp, M., Gomez, R. M., Murphy, M., Tran, H., and McGaw, J.: Evolution of observed ozone, trace gases, and meteorological variables over Arrival Heights, Antarctica (77.8○S, 166.7○E) during the 2019 Antarctic stratospheric sudden warming, Tellus B: Chemical and Physical Meteorology, 73, 1–18, https://doi.org/10.1080/16000889.2021.1933783, 2021.

Solomon, S.: Stratospheric ozone depletion: A review of concepts and history, Rev. Geophys., 37, 275–316, 500   https://doi.org/10.1029/1999RG900008, 1999.

Solomon, S., Garcia, R. R., Rowland, F. S., and Wuebbles, D. J.: On the depletion of Antarctic ozone, Nature, 321, 755–758, 1986.

Solomon, S., Borrmann, S., Garcia, R. R., Portmann, R., Thomason, L., Poole, L. R., Winker, D., and McCormick, M. P.: Heterogeneous chlorine chemistry in the tropopause region, J. Geophys. Res., 102, 21 411–21 429, 1997.

Solomon, S., Portmann, R. W., Sasaki, T., Hofmann, D. J., and Thompson, D. W. J.: Four decades of ozonesonde measurements over 505   Antarctica, J. Geophys. Res., 110, D21311, https://doi.org/10.1029/2005JD005917, 2005.

Solomon, S., Kinnison, D., Bandoro, J., and Garcia, R.: Simulation of polar ozone depletion: An update, J. Geophys. Res., 120, 7958–7974, https://doi.org/10.1002/2015JD023365, 2015.

Spang, R., Hoffmann, L., Müller, R., Grooß, J.-U., Tritscher, I., Höpfner, M., Pitts, M., Orr, A., and Riese, M.: A climatology of polar stratospheric cloud composition between 2002 and 2012 based on MIPAS/Envisat observations, Atmos. Chem. Phys., 18, 5089–5113, 510   https://doi.org/10.5194/acp-18-5089-2018, 2018.

Stone, K. A., Solomon, S., Kinnison, D. E., and Mills, M. J.: On Recent Large Antarctic Ozone Holes and Ozone Recovery Metrics, Geophys. Res. Lett., 48, https://doi.org/10.1029/2021GL095232, 2021.

Strahan, S. E. and Douglass, A. R.: Decline in Antarctic Ozone Depletion and Lower Stratospheric Chlorine Determined From Aura Microwave Limb Sounder Observations, Geophys. Res. Lett., 45, 382–390, https://doi.org/https://doi.org/10.1002/2017GL074830, 2018.

515   Struthers, H., Bodeker, G. E., Austin, J., Bekki, S., Cionni, I., Dameris, M., Giorgetta, M. A., Grewe, V., Lefèvre, F., Lott, F., Manzini, E., Peter, T., Rozanov, E., and Schraner, M.: The simulation of the Antarctic ozone hole by chemistry-climate models, Atmos. Chem. Phys., 9, 6363–6376, https://doi.org/10.5194/acp-9-6363-2009, 2009.

Tilmes, S., Müller, R., Salawitch, R. J., Schmidt, U., Webster, C. R., Oelhaf, H., Russell III, J. M., and Camy-Peyret, C. C.: Chemical ozone loss in the Arctic winter 1991–1992, Atmos. Chem. Phys., 8, 1897–1910, 2008.

520   Tilmes, S., Richter, J. H., Kravitz, B., MacMartin, D. G., Glanville, A. S., Visioni, D., Kinnison, D. E., and Müller, R.: Sensitivity of total column ozone to stratospheric sulfur injection strategies, Geophys. Res. Lett., 48, e2021GL094058, https://doi.org/10.1029/2021GL094058, 2021.

Tritscher, I., Grooß, J.-U., Spang, R., Pitts, M. P., Poole, L. R., Müller, R., and Riese, M.: Lagrangian simulation of ice particles and resulting dehydration in the polar winter stratosphere, Atmos. Chem. Phys., 19, 543–563, https://doi.org/10.5194/acp-19-543-2019, 2019.

525   Tritscher, I., Pitts, M. C., Poole, L. R., Alexander, S. P., Cairo, F., Chipperfield, M. P., Grooß, J.-U., Höpfner, M., Lambert, A., Luo, B. P., Molleker, S., Orr, A., Salawitch, R., Snels, M., Spang, R., Woiwode, W., and Peter, T.: Polar Stratospheric Clouds: Satellite Observations, Processes, and Role in Ozone Depletion, Rev. Geophys., 59, https://doi.org/10.1029/2020RG000702, 2021.

Várai, A., Homonnai, V., Jánosi, I. M., and Müller, R.: Early signatures of ozone trend reversal over the Antarctic, Earth's Future, 3, 95–109, https://doi.org/10.1002/2014EF000270, 2015.

530 Vömel, H., Oltmans, S. J., Hofmann, D. J., Deshler, T., and Rosen, J. M.: The evolution of the dehydration in the Antarctic stratospheric vortex, Geophys. Res. Lett., 100, 13 919 – 13 926, 1995.

von der Gathen, P., Kivi, R., Wohltmann, I., Salawitch, R. J., and Rex, M.: Climate change favours large seasonal loss of Arctic ozone, Nat. Commun., 12, 3886, https://doi.org/10.1038/s41467-021-24089-6, 2021.

von Hobe, M., Grooß, J.-U., Günther, G., Konopka, P., Gensch, I., Krämer, M., Spelten, N., Afchine, A., Schiller, C., Ulanovsky, A., Sitnikov,
535   N., Shur, G., Yushkov, V., Ravegnani, F., Cairo, F., Roiger, A., Voigt, C., Schlager, H., Weigel, R., Frey, W., Borrmann, S., Müller, R., and Stroh, F.: Evidence for heterogeneous chlorine activation in the tropical UTLS, Atmos. Chem. Phys., 11, 241–256, 2011.

Ward, M. K. M. and Rowley, D. M.: Kinetics of the ClO + CH_3O_2 reaction over the temperature range $T = 250$–298 K, Phys. Chem. Chem. Phys., 18, 13 646–13 656, https://doi.org/10.1039/C6CP00724D, 2016.

Weber, M., Arosio, C., Coldewey-Egbers, M., Fioletov, V. E., Frith, S. M., Wild, J. D., Tourpali, K., Burrows, J. P., and Loyola, D.: Global
540   total ozone recovery trends attributed to ozone-depleting substance (ODS) changes derived from five merged ozone datasets, Atmos. Chem. Phys., 22, 6843–6859, https://doi.org/10.5194/acp-22-6843-2022, 2022.

Wegner, T., Grooß, J.-U., von Hobe, M., Stroh, F., Sumińska-Ebersoldt, O., Volk, C. M., Hösen, E., Mitev, V., Shur, G., and Müller, R.: Heterogeneous chlorine activation on stratospheric aerosols and clouds in the Arctic polar vortex, Atmos. Chem. Phys., 12, 11 095–11 106, https://doi.org/10.5194/acp-12-11095-2012, 2012.

545 WMO: Scientific assessment of ozone depletion: 2022, GAW Report No. 278, Geneva, Switzerland, 2022.

Wohltmann, I., Lehmann, R., and Rex, M.: A quantitative analysis of the reactions involved in stratospheric ozone depletion in the polar vortex core, Atmos. Chem. Phys., 17, 10 535–10 563, https://doi.org/10.5194/acp-17-10535-2017, 2017.

Wohltmann, I., von der Gathen, P., Lehmann, R., Maturilli, M., Deckelmann, H., Manney, G. L., Davies, J., Tarasick, D., Jepsen, N., Kivi, R., Lyall, N., and Rex, M.: Near complete local reduction of Arctic stratospheric ozone by severe chemical loss in spring 2020, Geophys.
550   Res. Lett., 47, https://doi.org/10.1029/2020GL089547, 2020.

Zafar, A. M., Müller, R., Grooß, J.-U., Robrecht, S., Vogel, B., and Lehmann, R.: The relevance of reactions of the methyl peroxy radical (CH_3O_2) and methylhypochlorite (CH_3OCl) for Antarctic chlorine activation and ozone loss, Tellus B: Chemical and Physical Meteorology, 70, 1–18, https://doi.org/10.1080/16000889.2018.1507391, 2018.

Zhong, W. and Haigh, J. D.: Improved Broadband Emissivity Parameterization for Water Vapor Cooling Rate Calculations, J. Atmos. Sci.,
555   52, 124–138, https://doi.org/10.1175/1520-0469(1995)052<0124:IBEPFW>2.0.CO;2, 1995.